

UNCLASSIFIED

Defense Technical Information Center
Compilation Part Notice

ADP020519

TITLE: Development of Nickel-Titanium Graded Composition
Components

DISTRIBUTION: Approved for public release, distribution unlimited

This paper is part of the following report:

TITLE: Proceedings of Solid Freeform Fabrication Symposium [15th] Held
in Austin, Texas on August 2-4, 2004

To order the complete compilation report, use: ADA440272

The component part is provided here to allow users access to individually authored sections
of proceedings, annals, symposia, etc. However, the component should be considered within
the context of the overall compilation report and not as a stand-alone technical report.

The following component part numbers comprise the compilation report:

ADP020456 thru ADP020536

UNCLASSIFIED

Development of Nickel-Titanium Graded Composition Components

M. S. Domack* and J. M. Baughman**

*NASA Langley Research Center, Hampton, VA 23681

**Lockheed Martin Space Operations, Hampton, VA 23681

Abstract

The potential of various manufacturing methods was evaluated for producing nickel-titanium graded composition material. The selected test case examined attachment brackets that join nickel-based metallic thermal protection systems to titanium-based launch vehicle structure. The proposed application would replace nickel-based components with graded composition components in an effort to alleviate service induced thermal stresses. Demonstration samples were produced by laser direct metal deposition, flat wire welding, and ultrasonic consolidation. Microstructure, general bond quality, and chemistry were evaluated for the components.

Introduction

The ability to fabricate bulk materials with graded composition offers the potential for unique solutions to engineering problems and offers advantages over conventional materials and traditional composites. Research and development of functionally graded materials has largely focused on surface coatings or modifications of surface layers to enhance wear, optical, or electrical properties. Application of functional grading in bulk form offers the ability to create components with tailored chemistries or microstructures which enables properties to be selectively enhanced in critical regions. The current study examines the potential of various manufacturing methods for producing bulk material with composition graded from nickel-based Inconel 718 to titanium alloy Ti - 6Al - 4V (Ti-6-4). The test case for application of such material is an attachment bracket that joins nickel-based metallic thermal protection systems to titanium-based launch vehicle structure. The goal of the current study was to evaluate the compatibility of each method with the materials selected, examine the resulting microstructures and chemistries, and characterize any reaction products.

Metallic thermal protection systems (TPS) under development offer potentially greater durability than ceramic tile systems. One design, shown in Figure 1, employs attachment brackets to join a hot service aeroshell to an integrally stiffened tank structure [1, 2]. In this concept the attachment bracket is made from Inconel 718 strip approximately 4 in. long, 1 in. wide, and 0.020 in. thick, with 0.5 in. long flanges at each end to facilitate brazing to the Inconel 718 aeroshell and the Ti-6-4 tank structure. Thermal analysis indicates that temperatures at the Inconel end would reach 1800°F and be in the range of 400-500°F at the Ti end. The limitation of this design is accommodation of thermal expansion during flight without generating excessive bending or shear loads that impact the service life of the attachment bracket. Replacement of the Inconel 718 attachment clip with one produced from a graded composition component may reduce the stress concentrations.

Three manufacturing routes were evaluated for producing a composition graded from Inconel 718 to Ti-6-4 in bulk form: laser direct metal deposition, flat wire welding, and ultrasonic consolidation. All of these processes are layer-additive but differ in the feedstock and method of energy input used to consolidate material. Each process offers unique manufacturing flexibility and process benefits. Laser direct metal deposition consolidates deposited metal

powder using a high energy laser beam. Flat wire welding is a pulsed laser based method of joining sequential layers of metallic wire. Ultrasonic consolidation is a solid state process that consolidates foil layers by application of frictional energy under load.

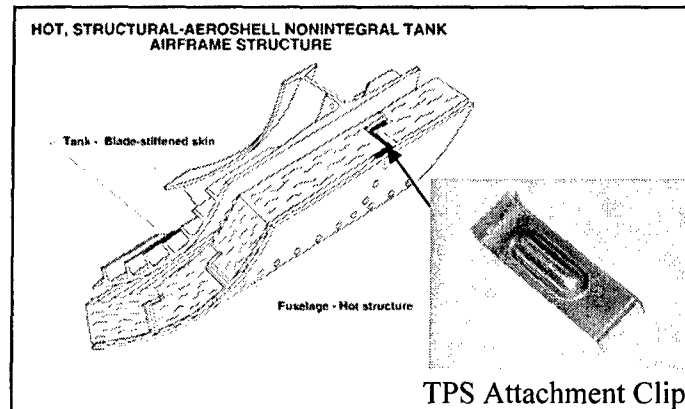


Figure 1. Concept drawing of a metallic thermal protection system employing attachment clips to join a hot Inconel 718 aeroshell to a Ti-6-4 integrally stiffened tank structure.

Materials and Processes

Laser direct metal deposition trials were conducted with the Laser Engineered Net Shape (LENS) process developed at Sandia National Laboratories [3]. The LENS process, shown schematically in Figure 2, is a layer additive powder deposition process that consolidates powder layers with a laser operated in continuous beam mode. The LENS process employs multiple nozzles to feed elemental and pre-alloyed powders to produce nearly continuous composition gradients. A wall-shaped build in progress is shown in Figure 3. The deposits for this study were produced on Ti-6-4 base plates from powders of Ti-6-4 and/or Inconel 718. The

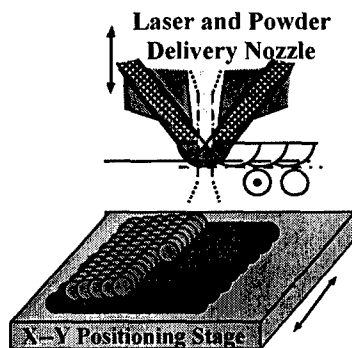


Figure 2. Schematic of the laser engineered net shape (LENS) process.

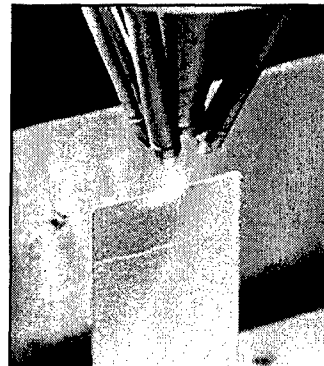


Figure 3. Wall-shaped build in progress using the LENS process.

chemistries for the supplied powders are provided in Table 1. Deposits were produced from Ti-6-4 and Inconel 718 in order to establish deposition parameters. A series of constant composition deposits were produced from pre-mixed powder blends, with the composition adjusted in steps of 10% by volume from 100% Ti-6-4 to 100% Inconel 718, to investigate deposition performance for specific alloy combinations. Deposits with continuous composition

gradients were achieved by simultaneously adjusting the feed rate of each powder in order to achieve a target composition profile and the deposition parameters in order to control the build quality. Deposit geometries included walls, columns, and cylinders.

Table 1. Chemical compositions of Inconel 718 and Ti-6-4 powder in weight percent.

Element	Inconel 718	Ti-6-4
Iron	18.4	0.091
Nickel	52.4	0.020
Chromium	19.1	0.0074
Columbium	5.02	<0.002
Tantalum	<0.004	<0.004
Molybdenum	3.15	0.0053
Titanium	1.00	88.8
Aluminum	0.32	6.29
Vanadium	0.010	4.17
Oxygen	0.043	0.081

Flat wire welding trials were performed using the Precision Metal Deposition (PMD™) process developed by H&R Technology, Inc. [4]. The PMD™ process, shown schematically in Figure 4, is a pulsed laser-based metal additive fabrication process. The PMD™ process fuses solid flat metal wire onto a substrate without the need to create a molten pool of metal on the substrate. As a result, metal parts can be fabricated with an order of magnitude less heat input than continuous-beam laser metal deposition processes, yielding parts with minimal distortion and improved metallurgical characteristics. Composition gradients in bulk components can be tailored by adjusting the stacking sequence of wires of different composition. The current study evaluated the compatibility of the PMD™ process with Inconel 718 and Ti-6-4 as well as the interactions that occur when the alloys are combined in a gradient composition component.

All of the flat wire welded deposits were produced on Inconel 718 base plates using Ti-6-4 and/or Inconel 718 rectangular cross section wire, as summarized in Table 2, and included three or four layers with three wires deposited side-by-side in each layer. Deposits were produced from Inconel 718 wire, 0.018 in. thick and 0.028 in. wide, in order to establish process parameters. In addition, deposits were produced from Ti-6-4 wire in order to establish process parameters and to investigate interactions with the Inconel 718 base plate. The Ti-6-4 wire used had dimensions 0.016 in. thick and 0.027 in. wide or 0.005 in. thick and 0.028 in. wide. Graded composition deposits were made by depositing three layers of 0.005 in. thick Ti-6-4 wire followed by one layer of Inconel 718 wire.

Ultrasonic consolidation (UC), developed by Solidica, Inc., is a micro-friction solid-state process used to join foil gage feedstock to build parts in a layer additive fashion [5]. The UC process, shown schematically in Figure 5, produces metallurgical bonds between layers without melting. The layer being added is translated against the previous build at ultrasonic frequency and low amplitude resulting in fracture and displacement of surface oxides. The clean surfaces

are brought together at a temperature typically less than half the material melting temperature and under applied load to promote atomic diffusion. The sonotrode is rotated across the build surface to continuously consolidate foil strip.

Table 2. Materials and Configuration used for Inconel 718 and Ti-6-4 Deposits.

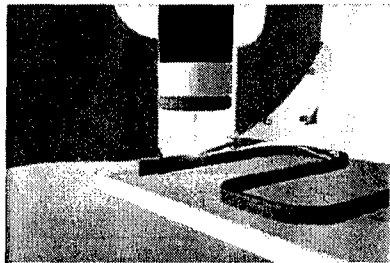


Figure 4. Schematic of the Precision Metal Deposition (PMD™) Process.

Sample Number	Alloy Deposited	Substrate Material	Number of Layers	Wires per Layer	Wire Dimensions	
					Thickness (in.)	Width (in.)
1-1	In 718	In 718	3	3	0.018	0.028
1-2	In 718	In 718	3	3	0.018	0.028
1-3	In 718	In 718	3	3	0.018	0.028
2-1	Ti-6-4	In 718	3	3	0.016	0.027
2-2	Ti-6-4	In 718	3	3	0.005	0.028
2-3	Ti-6-4	In 718	3	3	0.005	0.028
3-1	Ti-6-4 + In 718 (Layer4)	In 718	4	3	0.005 + 0.018	0.028
3-2	Ti-6-4 + In 718 (Layer4)	In 718	4	3	0.005 + 0.018	0.028

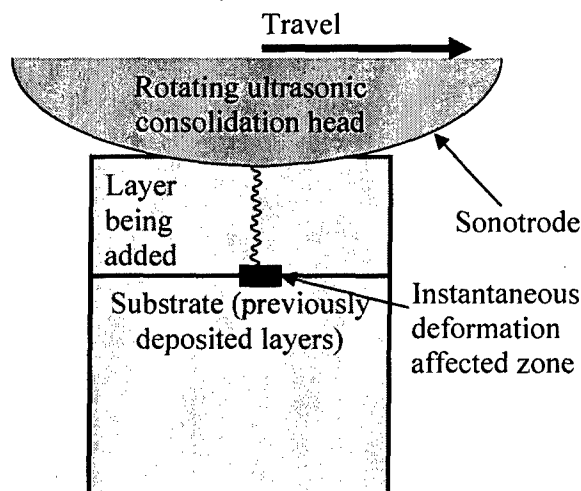


Figure 5. Schematic of the ultrasonic consolidation process.

Nickel and titanium alloys are suitable for ultrasonic consolidation, but the process is not mature for these materials. Samples were produced for this study from pure Ni and commercially pure (CP) Ti foils to demonstrate the feasibility of developing metallurgical bonding without undesirable metallurgical interaction. For this feasibility study, static joining of small 0.24 in. x 0.6 in. samples was attempted by using a modified spot welding system equipped with a knurled tool steel sonotrode, rather than the rolling strip application. Samples were

produced from pure Ni and from CP Ti in order to establish processing parameters. Graded samples were produced by layering Ni and CP Ti foils in the sequence Ni-Ni-Ni-Ti-Ni-Ti-Ti-Ti. The CP Ti foil was 0.002 in. thick rolled foil, and the Ni foil was 0.002 in. thick electrodeposited foil.

Analysis of all samples produced for this study employed standard metallographic techniques for sectioning and polishing. However, etching procedures were tailored for each product and material combination in order to examine bond lines, evaluate material interactions, and reveal grain structures. Chemical analysis was evaluated by direct current plasma spectroscopy for bulk samples and by energy dispersive x-ray analysis of specimen sections.

Results and Discussion

Laser Direct Metal Deposition

Test samples produced by the LENS process for this study are shown in Figure 6. During building of the Ti-6-4 wall (2.5 in. x 4.0 in.) power was adjusted to control rippling and smooth the surface. Power and feed rate were adjusted during building of the series of Inconel 718 walls (2.5 in. wide x 2.5 in. tall max.) in order to reduce rippling, warping, and separation from the base plate. The Inconel 718 deposits generally had a smoother surface than that of the Ti-6-4 deposits. Metallographic sections of the Inconel 718 wall, shown in Figure 7 etched with a solution of HNO₃ and HCl, exhibited banding associated with the laser passes. The microstructure was primarily a fine scale dendritic solidification structure with coarser dendrites noted near the surface of the deposit. The Ti-6-4 wall, shown in Figure 8 etched with Keller's reagent, exhibited significant surface roughness characterized by serrations that were on the scale of the deposited powder layer. Residual powder particles were loosely adherent to the surface of the deposit. The microstructure exhibited large columnar grains, prior- β grain boundaries, and fine alpha laths within the grains. The columnar grain structure indicates that epitaxial growth of β likely occurred during laser consolidation of the added powder layer with transformation of β to α during cooling.

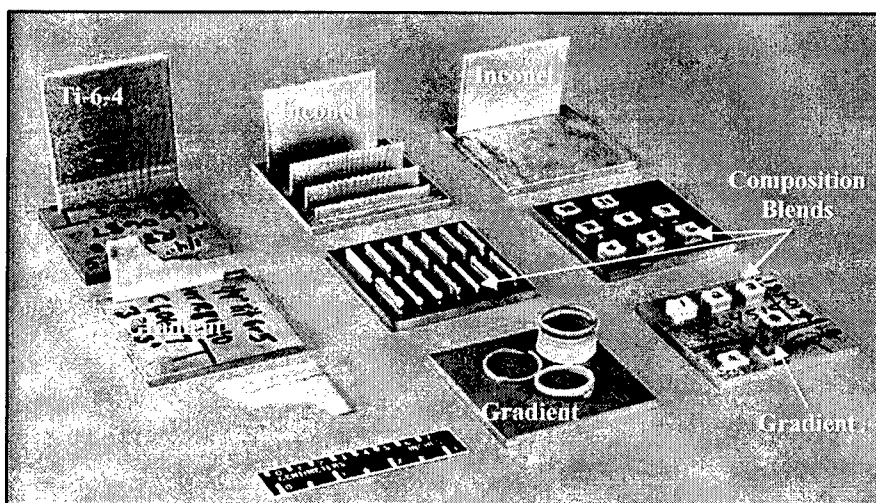


Figure 6. LENS samples produced from Ti-6-4 and Inconel 718 powders.

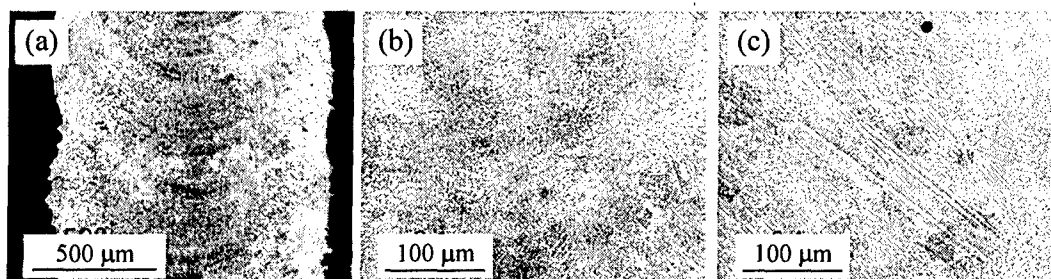


Figure 7. Microstructure of the Inconel 718 deposit illustrating (a) laser pass boundaries, (b) fine dendrite structure, and (c) coarse dendrite structure.

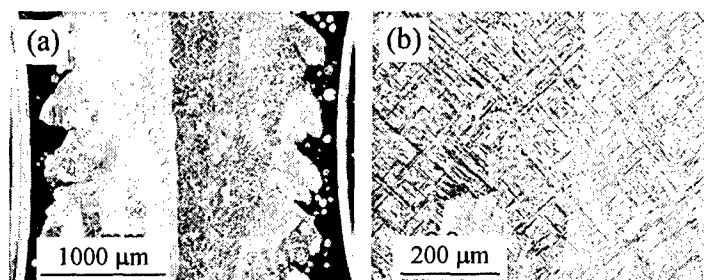


Figure 8. Microstructure of the Ti-6-4 deposit illustrating (a) surface roughness, large columnar grain structure, and (b) alpha laths.

Constant composition blends of the two materials were deposited to build walls 1 in. wide x 0.5 in. tall and columns 0.375 x 0.375 x 0.5 in. tall. Cracking was observed in the walls when the composition blend was 50% each Ti-6-4 and Inconel 718 and in the columns when the blend was 40% Ti-6-4 and 60% Inconel 718. Chemical analysis of the constant composition blend column samples is summarized in Table 3 for the various powder blends. The results indicated that the deposits targeted to be 100% Ti-6-4 and 100% Inconel 718

Table 3. Chemical compositions of the constant composition blend column samples in weight percent.

Element	Target Powder Blend (volume percent Ti-6-4 – volume percent Inconel 718)										
	100-0	90-10	80-20	70-30	60-40	50-50	40-60	30-70	20-80	10-90	0-100
Iron	3.37	4.60	5.83	7.62	9.36	10.9	11.1	12.5	13.8	14.5	15.9
Nickel	10.1	13.7	17.5	22.3	27.6	32.2	32.6	36.8	40.3	42.9	45.7
Chromium	3.64	4.98	6.34	8.24	10.1	11.7	11.8	13.3	14.7	14.9	16.3
Columbium	0.99	1.36	1.65	2.07	2.49	2.89	3.15	3.40	3.75	4.29	4.36
Tantalum	<0.004	<0.004	<0.004	<0.004	<0.004	<0.004	<0.004	<0.004	<0.004	<0.004	<0.004
Molybdenum	0.58	0.80	1.01	1.33	1.61	1.80	1.92	2.13	2.29	2.55	2.78
Titanium	72.3	66.1	59.9	51.7	43.0	35.6	34.7	28.0	22.1	18.2	12.9
Aluminum	5.05	4.80	4.42	3.81	3.28	2.70	2.67	2.18	1.66	1.42	1.05
Vanadium	3.36	3.06	2.74	2.37	2.00	1.71	1.64	1.17	0.82	0.69	0.47
Oxygen	0.073	0.072	0.069	0.066	0.064	0.060	0.062	0.059	0.053	0.051	0.049

contained 10-20% of the other material, which may reflect residual powder from prior deposits. The compositions of the remaining powder blends differed by 10-20% from calculated compositions based on target powder volume percent, suggesting that further development is needed in powder feed control. The deposits with target powder blend of 60-80% Inconel 718 agreed best with calculated composition. X-ray chemical analysis of the short column deposit with target blend of 10% Ti-6-4 and 90% Inconel 718, summarized in Figure 9, revealed a complex solidification structure with significant elemental segregation. The backscattered scanning electron microscope image shows a coarse dendrite structure with partitioning of nickel and iron, circular aluminum and chromium rich inclusions, and occasional titanium rich inclusions.

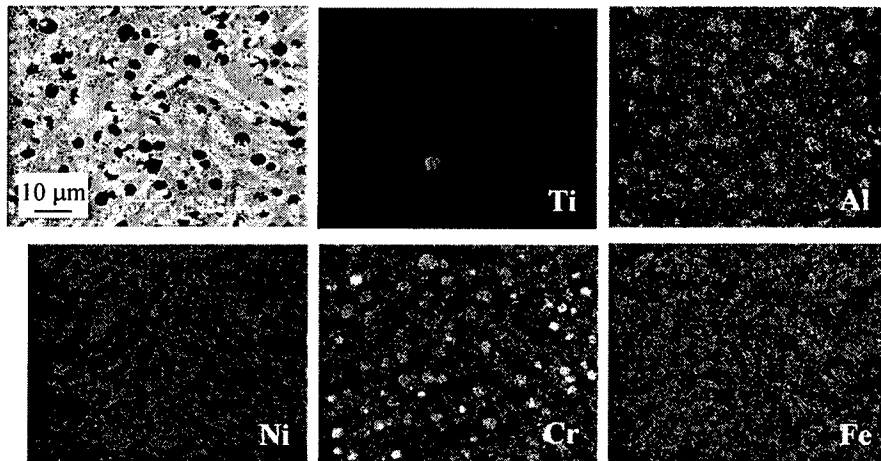


Figure 9. X-ray chemical maps of the column deposit with target powder blend of 10% Ti-6-4 and 90% Inconel 718.

The graded composition deposits developed macroscopic cracks (Figure 10) before the full transition from Ti-6-4 to Inconel 718 was achieved. The 2.5 in. wide wall developed a large crack when the composition reached a target mix of approximately 58% Ti-6-4 and 42% Inconel 718, based on powder feed control, with the crack propagating to complete fracture of the build during shutdown and removal of the sample. The column (0.375 in. x 0.375 in. x 0.98 in.) developed a crack when the target blend was about 40% Ti-6-4 and 60% Inconel 718. The build was continued to completion but additional cracks developed. Both deposits exhibited

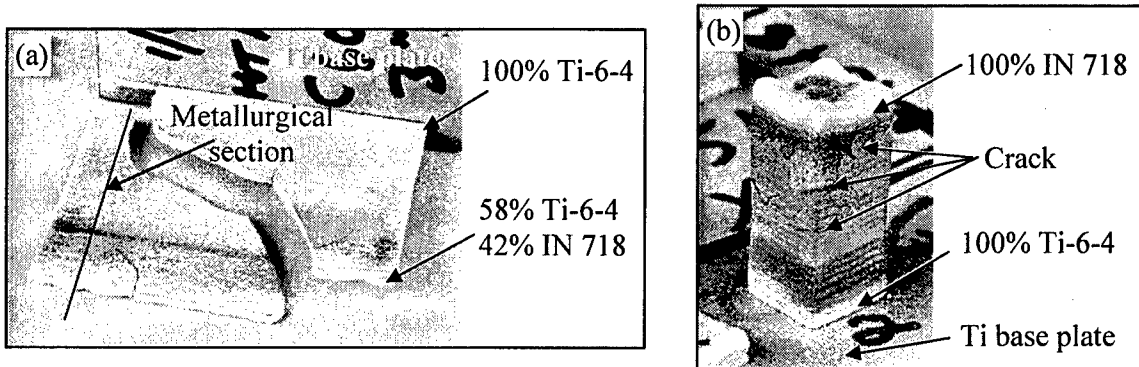


Figure 10. Graded composition (a) wall and (b) column deposits illustrating macroscopic cracks.

significant secondary cracking as well. The microstructures were similar for the column and wall and revealed that the cracks were not directly linked to metallurgical features. Macroscopic banding was observed, as shown in Figure 11a, likely due to the laser passes used to consolidate each powder layer. The sample was etched with an HNO_3/HCl solution + Keller's reagent. The microstructures were fully dendritic with coarser structure in the lighter bands. Residual Ti-6-4 powder particles that were not melted during processing were observed near the surfaces. The primary fracture surface of the wall (Figure 12) exhibited brittle, cleavage fracture features and residual Ti-6-4 powder particles. A reaction layer was visible around the Ti-6-4 powder particles both in cross section (Figure 11c) and on the fracture surface (Figure 12c).

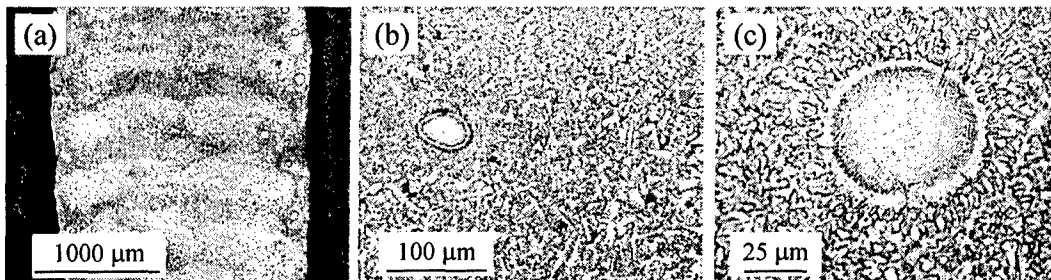


Figure 11. Metallurgical section of the graded composition wall deposit illustrating (a) microstructure banding, (b) dendrite structure, and (c) residual Ti-6-4 powder.

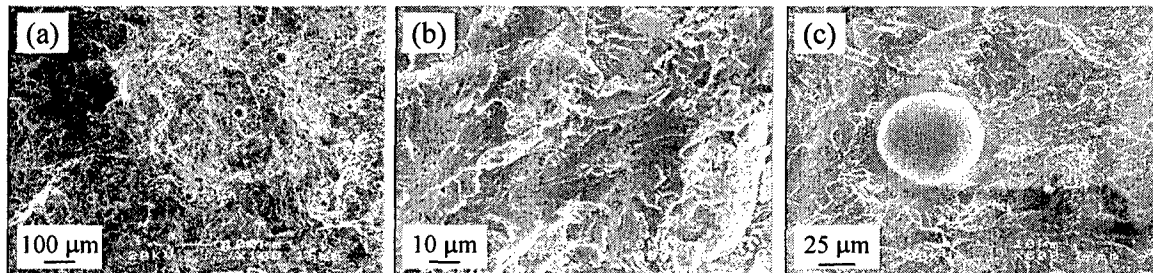


Figure 12. Fracture surface of (a) the graded composition wall deposit illustrating (b) brittle fracture features and (c) exposed residual Ti-6-4 powder.

Flat Wire Welding

Samples produced by the PMDTM flat wire welding process, shown in Figure 13, exhibited distinct wire layers (Figure 13a) and solidification fronts (Figure 13b) which were associated with the laser passes along the three wires in each layer. The Inconel 718 deposits were well integrated with the base plate but the Ti-6-4 and Ti-6-4/Inconel 718 deposits exhibited macroscopic cracking and separation at the base plate interface (Figure 13c). The Ti-6-4/Inconel 718 deposits also exhibited cracking through the layers of the deposit.

Metallurgical sections of the Inconel 718 deposit (Figure 14 etched with Kalling's reagent) showed full consolidation between the wire layers and banding associated with the laser passes. The microstructure exhibited large elongated grains that spanned the laser pass boundaries and were generally elongated in the through-thickness direction (Figure 14). Occasional porosity was also observed. A region of mixing was observed at the base plate interface that penetrated up to 300 μm into the base plate.

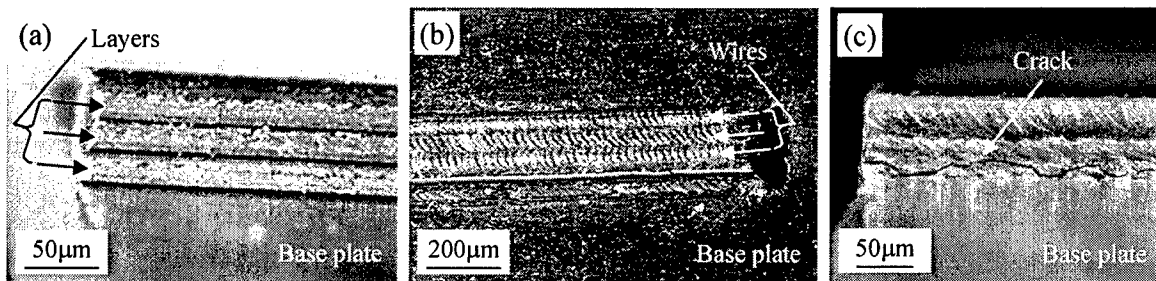


Figure 13. Typical appearance of the flat wire welded samples, illustrating (a) three layers, (b) solidification fronts along the three wires in each layer, and (c) cracking at the base of the Ti-6-4 deposits.

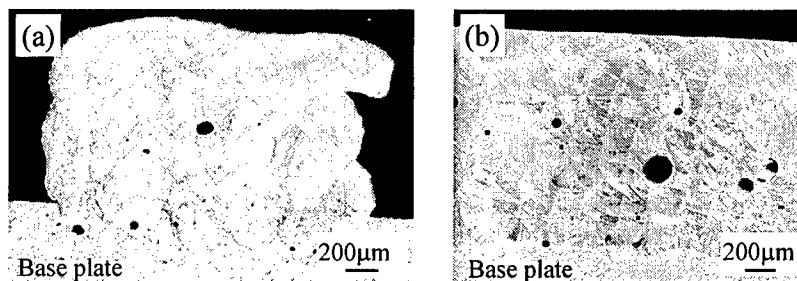


Figure 14. Metallurgical (a) cross and (b) longitudinal sections of Inconel 718 deposit built on Inconel 718 base plate showing solidification fronts, grain structure, and porosity.

Metallurgical sections of the Ti-6-4 deposit (Figure 15 etched with Kalling's + Flick's reagents) exhibited distinct boundaries between wire layers with variations in the microstructure of each layer. A nearly continuous crack was observed at the base plate interface with numerous secondary cracks through the first Ti-6-4 layer. The bottom Ti-6-4 layer was reduced in thickness compared with the second and third layers and also exhibited regions of mixing with the Inconel 718. A reaction layer was observed at the base plate interface, appearing as a 5 µm thick band, bordered by a 25-100 µm thick brittle fracture region.

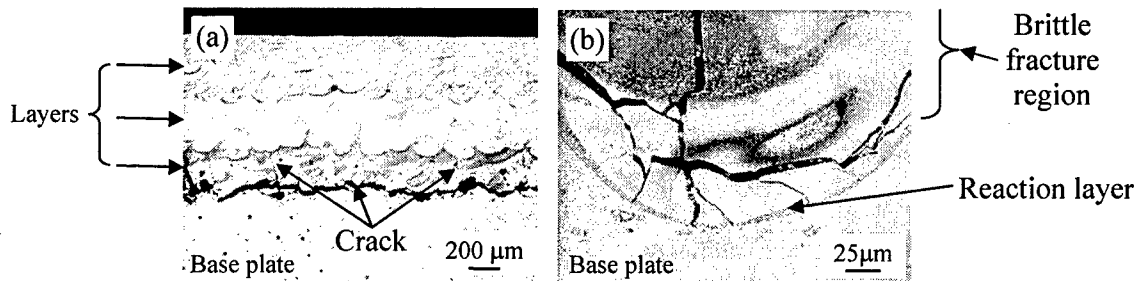


Figure 15. Metallurgical section of Ti-6-4 deposit built on Inconel 718 base plate showing (a) distinct wire layers, cracking, (b) the reaction layer and brittle fracture region.

The Ti-6-4 / Inconel 718 deposits exhibited more significant cracking at the base plate with some separation of the deposit, as shown in Figure 16. Metallurgical sections revealed distinct boundaries between the top Ti-6-4 wire layer and the Inconel 718 wire layer but the

boundaries between individual Ti-6-4 layers were not as clear. Some evidence of mixing as well as secondary cracking was observed in the lower portion of the Ti-6-4 region. Additional mixing was observed at the interface between the Ti-6-4 layers and the Inconel 718 layer. Reaction layers that were approximately 5 μm thick (Figure 17) were observed at the interface between the Ti-6-4 layers and both the Inconel 718 base plate and wire. The reaction layer was similar in appearance to that observed in the Ti-6-4 deposit.

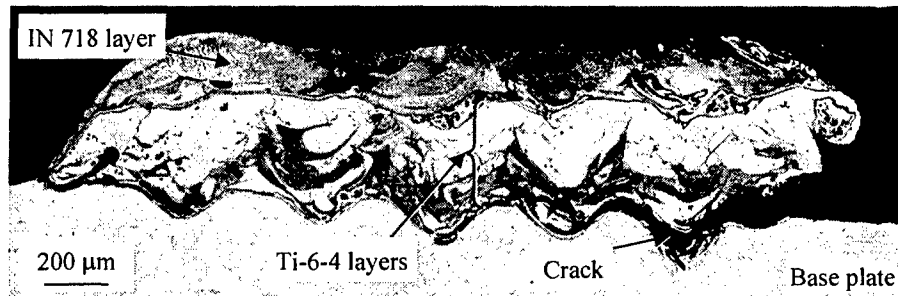


Figure 16. Metallurgical section of Ti-6-4 / Inconel 718 deposit built on Inconel 718 base plate. Section was etched with Kalling's and Kroll's reagents.

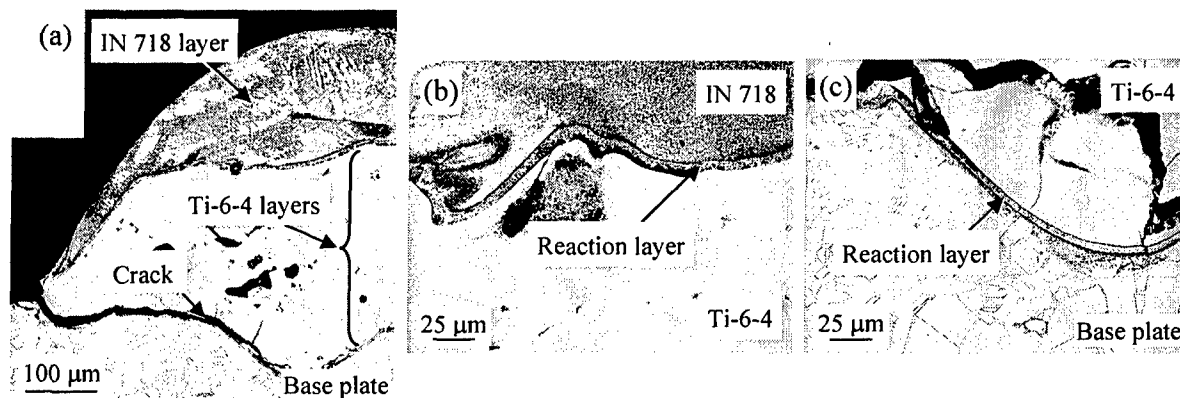


Figure 17. Metallurgical section of Ti-6-4/Inconel 718 deposit illustrating (a) cracking at the base plate interface and reaction layers between the Ti-6-4 wire and (b) the Inconel 718 wire and (c) the base plate. Section was etched with Kalling's reagent.

At higher magnification the reaction layer appeared to be a nearly featureless band, approximately 5 μm thick, as shown in Figure 18. The reaction layer shown has formed around a lobe of Inconel 718 drawn into the Ti-6-4 layer during interlayer mixing. Chemical analysis by energy dispersive spectroscopy was performed stepwise along a line spanning from Inconel 718 at the interior of the lobe to the surrounding Ti-6-4 layer. Semi-quantitative analysis demonstrated a gradient decreasing in Ni, Fe, and Cr and increasing in Ti and Al, but was not sensitive enough to fully quantify the chemistry. Crystallographic analysis and fully quantitative x-ray analysis of the reaction layer are underway and not included in this report.

The flat wire welding process was used to produce metallurgical mixing and bonding between Ti-6-4 and Inconel 718, although some cracking and material reaction occurred, which indicates the need for further process development. The pulse application of the laser in flat wire welding resulted in minimal segregation of elements as compared with the LENS process.

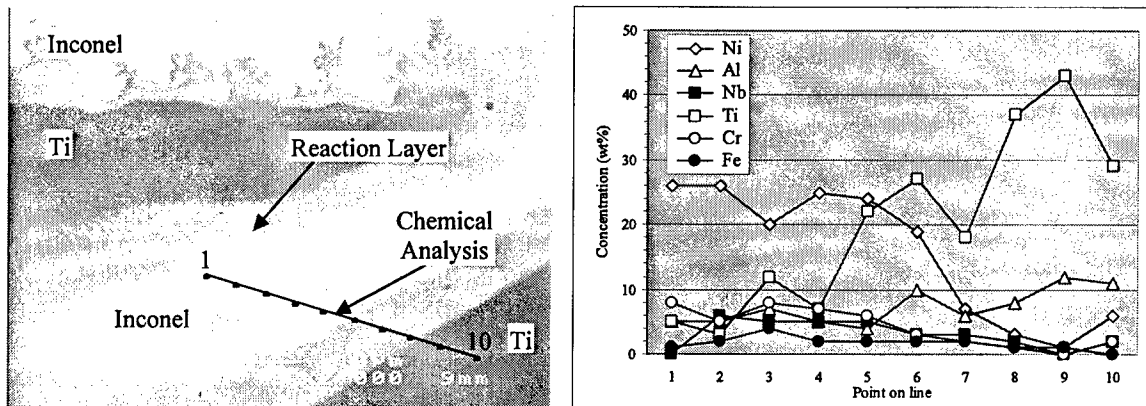


Figure 18. Detailed morphology and chemical analysis of a reaction layer formed in the region of mixing at the Ti-6-4 and Inconel 718 wire interface.

Ultrasonic Consolidation

The samples produced by ultrasonic consolidation exhibited indentations from the knurled surface of the sonotrode in the consolidated region, as shown in Figure 19. The free edges of the foil were flared due to peel loads manually applied by the manufacturer to ensure that the foils were bonded. The samples were sectioned along the length and across the remaining width as shown in Figure 19. The longitudinal section (Figure 20) revealed that there were residual indentations from the knurled surface of the sonotrode at each foil layer which prevented complete consolidation of the materials. The residual indentations are an experimental artifact associated with the spot weld application of the sonotrode. In the commercial process these voids are normally filled by plastic flow of material resulting from the rotation of the sonotrode. Regions of metallurgical bonding were identified on each sample for analysis.

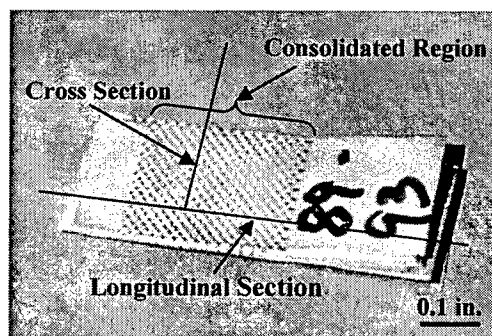


Figure 19. Typical ultrasonically-consolidated sample illustrating knurled surface in the consolidated region and flared foil edges.

Metallurgical bonding was achieved in samples produced from Ni and CP Ti foils. In both cases the microstructure of the foils remained unchanged by the consolidation process. The scanning electron microscope cross section image shown in Figure 21a includes five layers within a sample of ten Ni foil layers. The sample shown is in the as-polished condition. The triangular voids are residual indentations from the sonotrode. Metallurgical bonding (MB) is noted at the angled arrows and shown in greater detail in Figure 21b, which has been etched with

Kroll's reagent. The metallurgical bond line remained tightly closed after etching and exhibits some smearing of metal across the boundary. The Kroll's reagent also highlighted a centerline feature (C in Figure 21b) which is a remnant of the electrodeposition process used to produce the Ni foil.

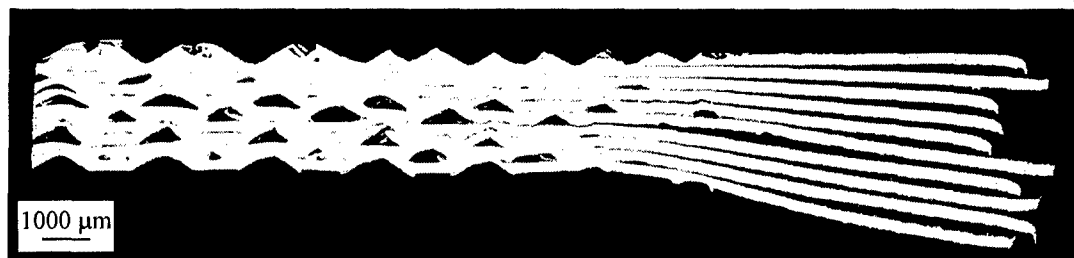


Figure 20. Longitudinal section illustrating residual voids from the knurled surface of the sonotrode. The example shown contains ten Ni foils in the as-polished condition.

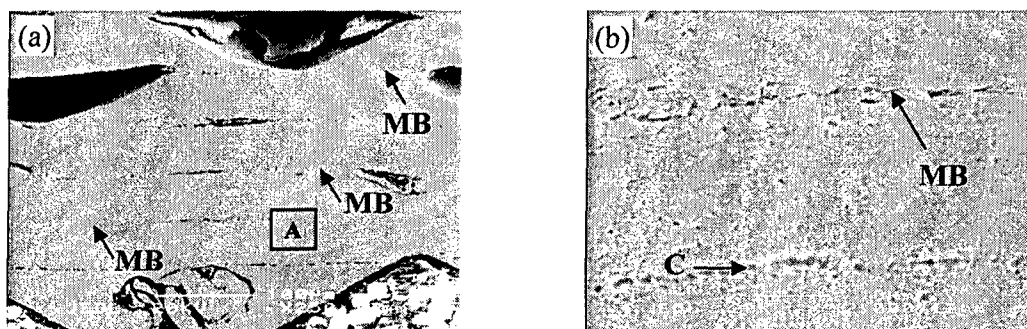


Figure 21. Metallurgical cross section of (a) an ultrasonically-consolidated sample containing ten Ni foils and (b) morphology of the bond line.

A portion of a UC sample containing eleven layers of CP Ti is shown in Figure 22 and has been lightly etched with a solution of HF, HNO₃, and lactic acid. Metallurgical bonds are apparent between three of the layers with no bonding at the triangular void. Higher magnification (Figure 22b) reveals that the etchant lightly attacked the bond line but the bond remained intact. In addition this view illustrates that the equiaxed alpha microstructure of the foil was unchanged during the consolidation process.

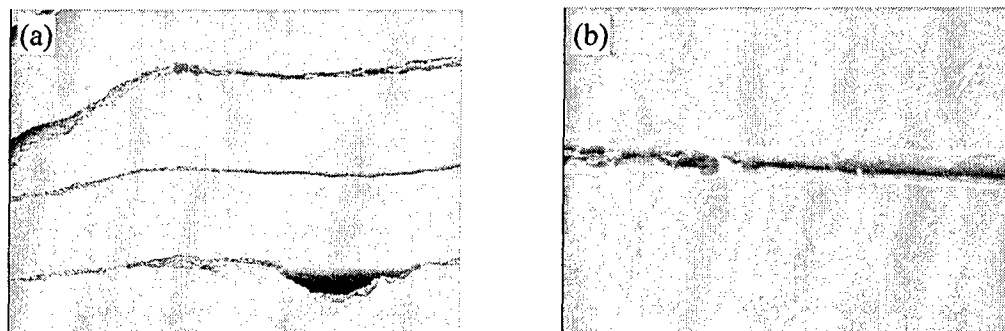


Figure 22. Metallurgical cross section of (a) an ultrasonically-consolidated sample containing eleven CP Ti foils and (b) morphology of the bond line.

The graded composition sample, shown in Figure 23, contained both Ni and Ti foils in the sequence Ni – Ni – Ni – Ti – Ni – Ti – Ti – Ti with the sonotrode applied between each layer. In the scanning electron microscope image shown in Figure 23a the Ni foils appear lighter than the Ti foils. Metallurgical bonding occurred between some layers but also evident are residual indentations from the sonotrode surface, occasional foil tearing, and separation of the topmost Ti foil. Higher magnification examination (Figure 23b) revealed that metallurgical bonding did occur between Ni and Ti foils, and was also observed between Ni-Ni and Ti-Ti pairs. In addition, the microstructure of each alloy appeared unchanged by the UC process.

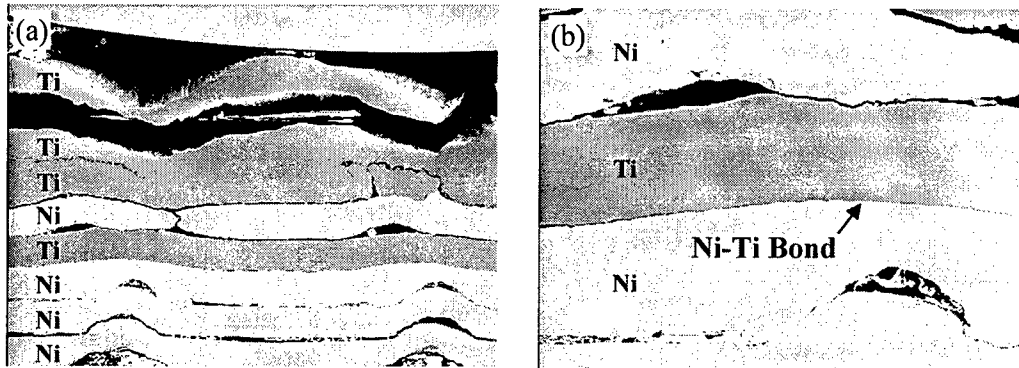


Figure 23. Metallurgical cross section of (a) an ultrasonically-consolidated sample containing Ni and CP Ti foils and (b) morphology of the bond line.

Higher magnification examination of the bond line between Ni and Ti foils revealed a reaction layer that was approximately 1 μm thick, as shown in Figure 24. Chemical analysis of the reaction layer and the surrounding Ni and Ti foils was performed by energy dispersive x-ray analysis in a scanning electron microscope and indicated (points 2-5) the presence of both Ni and Ti as well as higher concentrations of C and O than in the foils. Additional chemical analysis and x-ray crystallography are underway to determine the composition and structure of the reaction layer.

The ultrasonic consolidation process successfully created a metallurgical bond between CP Ti and pure Ni without melting either material. The extent and nature of material interaction requires further characterization but is clearly reduced compared with the flat wire welding process.

Analysis	C	N	O	Ti	Ni
1	4.9	1.9	2.6	1.3	89.3
2	25.4	5.7	14.1	21.4	33.5
3	19.4	4.9	13.6	30.1	32.0
4	23.4	5.6	17.7	30.6	22.7
5	6.3	1.5	7.2	65.9	19.2
6	3.1	10.4	19.7	64.6	2.1

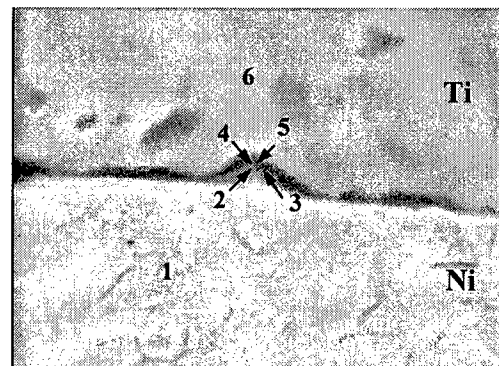


Figure 24. Chemical composition of the reaction layer in weight percent.

Concluding Remarks

The potential of three manufacturing methods was evaluated for producing bulk material with composition gradient from Ti-6-4 to Inconel 718. The methods were laser metal powder deposition, flat wire welding, and ultrasonic foil consolidation. All of the manufacturing methods require further development and additional characterization of produced samples before gradient composition materials can be reliably produced.

Graded composition samples produced by laser direct metal deposition exhibited significant macroscopic cracking for powder blends that contained 40-60% Inconel 718. Microstructures exhibited coarse dendrites and significant elemental segregation. The chemistries of deposits of fixed powder blends varied in accuracy by up to 20% compared with calculated target chemistry. Additional development of process parameters and powder feed control are necessary to ensure that target chemistry gradients are achieved without excessive material reactions.

The flat wire welding process resulted in layered deposits of Ti-6-4 and Inconel 718 wire that exhibited good mixing between the wire layers but also exhibited cracking at the alloy interface. A 5 μm thick reaction layer and region of brittle cracking were observed, but the degree of material reaction was significantly reduced compared with laser direct metal deposition.

Samples produced by ultrasonic consolidation demonstrated metallurgical bonding between pure Ni and commercially pure (CP) Ti foils without melting. Analysis of the bonded regions revealed a 1 μm reaction layer that was thinner than those observed for the other processes evaluated.

References

1. Blosser, M. L., Chen R. R., Schmidt, I. H., Dorsey, J. T., Poteet, C. C., Bird, R. K., and Wurster, K. E.; "Development of Advanced Metallic Thermal-Protection-System Prototype Hardware", *Journal of Spacecraft and Rockets*, Vol. 41, No. 2, March-April 2004, p. 183.
2. Blosser, M. L., "Advanced Metallic Thermal protection Systems for Reusable Launch Vehicles", PhD Thesis, University of Virginia, May 2000.
3. Sandia National Lab Laser Engineered Net Shaping CRADA No. SC96/01462, 1999.
4. Rabinovich, J., "Net Shape Manufacturing With Metal Alloys, *Advanced Materials and Processes*", Vol 161, No. 1, p. 47, January 2003.
5. White, D. R., "Ultrasonic Consolidation of Aluminum Tooling, *Advanced Materials and Processes*", Vol 161, No. 1, p. 64, January 2003.